PRODUCTION AND DECAY OF THE CHARGED D^* MESON IN e^+e^- ANNIHILATION AT 10 GeV CENTRE-OF-MASS ENERGY

ARGUS Collaboration

H. ALBRECHT, U. BINDER, G. DREWS, G. HARDER, H. HASEMANN, A. PHILIPP, W. SCHMIDT-PARZEFALL, H. SCHRÖDER, H.D. SCHULZ, F. SELONKE, R. WURTH
DESY, Hamburg, Germany

A. DRESCHER, B. GRÄWE, U. MATTHIESEN, H. SCHECK, J. SPENGLER, D. WEGENER
Institut für Physik, Universität Dortmund [1], *Germany*

R. HELLER, K.R. SCHUBERT, J. STIEWE, R. WALDI, S. WESELER
Institut für Hochenergiephysik, Universität Heidelberg [1], *Germany*

K.W. EDWARDS [2], W.R. FRISKEN [3], Ch. FUKUNAGA [3], M. GODDARD [3], P.C.H. KIM [4], R. KUTSCHKE [4], D.B. MacFARLANE [4], J.A. McKENNA [4], K. McLEAN [5], A. NILSSON [5], R.S. ORR [4], P. PADLEY [4], P.M. PATEL [5], J.D. PRENTICE [4], H.C.J. SEYWERD [4], B.J. STACEY [4], T.-S. YOON [4], J.C. YUN [2]
Institute of Particle Physics [6], *Canada*

R. AMMAR, D. COPPAGE, R. DAVIS, S. KANEKAL, N. KWAK
University of Kansas [7], *Lawrence, KS, USA*

P. BÖCKMANN [8], L. JÖNSSON, Y. OKU
Institute of Physics, University of Lund [9], *Sweden*

M. DANILOV, V. LUBIMOV, V. MATVEEV, N. NAGOVITSIN, V. RYLTSOV, Yu. SEMENOV, V. SHEVCHENKO, V. SOLOSHENKO, V. SOPOV, I. TICHOMIROV, Yu. ZAITSEV
Institute of Theoretical and Experimental Physics, Moscow, USSR

and

R. CHILDERS, C.W. DARDEN and H. GENNOW [10]
University of South Carolina [11], *Columbia, SC, USA*

Received 10 August 1984
Revised manuscript received 23 October 1984

[1] Supported by the Bundesministerium für Forschung und Technologie, Fed. Rep. Germany.
[2] Carleton University, Ottawa, Canada.
[3] York University, Downsview, Canada.
[4] University of Toronto, Toronto, Canada.
[5] McGill University, Montreal, Canada.
[6] Supported by the Natural Sciences and Engineering Research Council, Canada.
[7] Supported by the US National Science Foundation and a University of Kansas Faculty Improvement award.
[8] Present address: CERN, Geneva, Switzerland.
[9] Supported by the Swedish Research Council.
[10] On leave of absence from the University of Stockholm, Sweden.
[11] Supported by the US Department of Energy, under contract DE-AS09-80ER10690.

0370-2693/85/$ 03.30 © Elsevier Science Publishers B.V.
(North-Holland Physics Publishing Division)

Using the ARGUS detector at DORIS we have observed the production of the charged D^* meson in e^+e^- annihilation at a center of mass energy of 10 GeV. The D^* fragmentation function has been measured using the decay channels $D^{*+} \to D^0\pi^+$ and $D^0 \to K^-\pi^+$ and $K^-\pi^+\pi^+\pi^-$.

We find $\sigma \cdot Br$ for the channels $D^0 \to K^-\pi^+$ and $D^0 \to K^-\pi^+\pi^+\pi^-$ to be $(23.6 \pm 2.2 \pm 4.7)$ pb and $(51.0 \pm 4.6 \pm 15.5)$ pb respectively, and the ratio of branching ratios $Br(D^0 \to K^-\pi^+\pi^+\pi^-)/Br(D^0 \to K^-\pi^+) = 2.17 \pm 0.28 \pm 0.23$. In addition we measure the mass difference $M(D^{*+}) - M(D^0)$ to be $(145.46 \pm 0.07 \pm 0.03)$ MeV, and set an upper limit for $D^0 - \bar{D}^0$ mixing of 0.11.

High energy, non-resonant e^+e^- annihilation into hadrons proceeds through the formation of a primary $q\bar{q}$ pair which fragments into two hadron jets. Fast charmed hadrons will, in general, contain primary c quarks since the production of $c\bar{c}$ pairs in the fragmentation process is expected to be highly suppressed. The fragmentation process for c quarks can thus be studied by measuring the production of fast charmed mesons [1].

In this letter we present measurements of D^{*+} production (in the following we will omit explicit reference to charge conjugate states) at the Υ and Υ' resonance energies. The fragmentation function is compared to other experimental results and to two theoretical models, the ratio of the decay widths, and the cross section times branching ratios, of $D^0 \to K^-\pi^+$ and $D^0 \to K^-\pi^+\pi^+\pi^-$ are determined. We also present a determination of the D^{*+}, D^0 mass difference and an upper limit on $D^0 - \bar{D}^0$ mixing.

The data discussed here were collected with the ARGUS detector at the DORIS II storage ring at DESY. The event sample consists of 40 events/pb; 23% on the Υ, 67% on the Υ', and 10% on the continuum just below the Υ'.

The ARGUS detector is a solenoidal magnetic spectrometer having a field of 0.8 T. The main characteristics of the detector, and the triggering scheme used have been described elsewhere [2]. In the following analysis we have used only information from the drift chamber and from the time-of-flight counters.

The ARGUS drift chamber [3] is 2 m long and 0.9 m in radius. There are 5940 sense wires arranged in 36 concentric layers. Both drift time and the ionisation deposited are digitised. On average the spatial resolution is 170μ giving a momentum resolution of $\sigma_p/p = 0.012$ at 1 GeV/c.

In determining the specific ionization [dE/dx] of a track the truncated mean of the ionization deposited in a maximum of 36 chamber cells is used. This results in a resolution of $\sigma(dE)/dE = 0.042$. Fig. 1a shows a scatter plot of momentum versus dE/dx for a random selection of tracks traversing at least 20 chamber cells. The bands corresponding to π, K, p are clearly separated. Better than three standard deviation separation is achieved for π and K below 700 MeV/c, and for K and p below 1200 MeV/c.

Surrounding the drift chamber there is a system of time-of-flight [TOF] counters [4]. There are 64 scintillators, each 2 cm thick, in the barrel system and 48 in each end cap. In the barrel system the scintillators have a photomultiplier at each end, while those in the end cap are equipped with only one photomultiplier. In addition to digitising the time on each photomultiplier, the pulse height is also digitised to allow for offline correction of the timing. A time resolution of 220 ps is achieved in the barrel counters, and 230 ps in the end caps. Fib. 1b shows a scatter plot of momentum versus (mass)^2. The separation achieved is similar to that using the drift chamber.

For each track in an event a χ^2 for each mass hypothesis is calculated by adding the corresponding χ^2 values for the dE/dx and TOF measurements. The normalized probability for each mass hypothesis is then:

$$P_i = \exp(-\chi_i^2/2) \Big/ \sum \exp(-\chi_j^2/2), \quad i = \pi, K, p.$$

A track is considered a candidate for each mass hypothesis which gives an acceptable probability. Tracks giving an acceptable probability for more than one mass hypothesis enter into several mass combinations with equal weight. The effect of varying the probability cut in the range 0.01 to 0.03 was studied and the results of the analysis were found to be insensitive to the exact value chosen in this range.

We have identified charged D^* mesons by means of a well established procedure [5] which exploits the low Q value (5.8 MeV) of the decay $D^{*+} \to D^0\pi^+$. This gives very fine mass resolution in the mass differ-

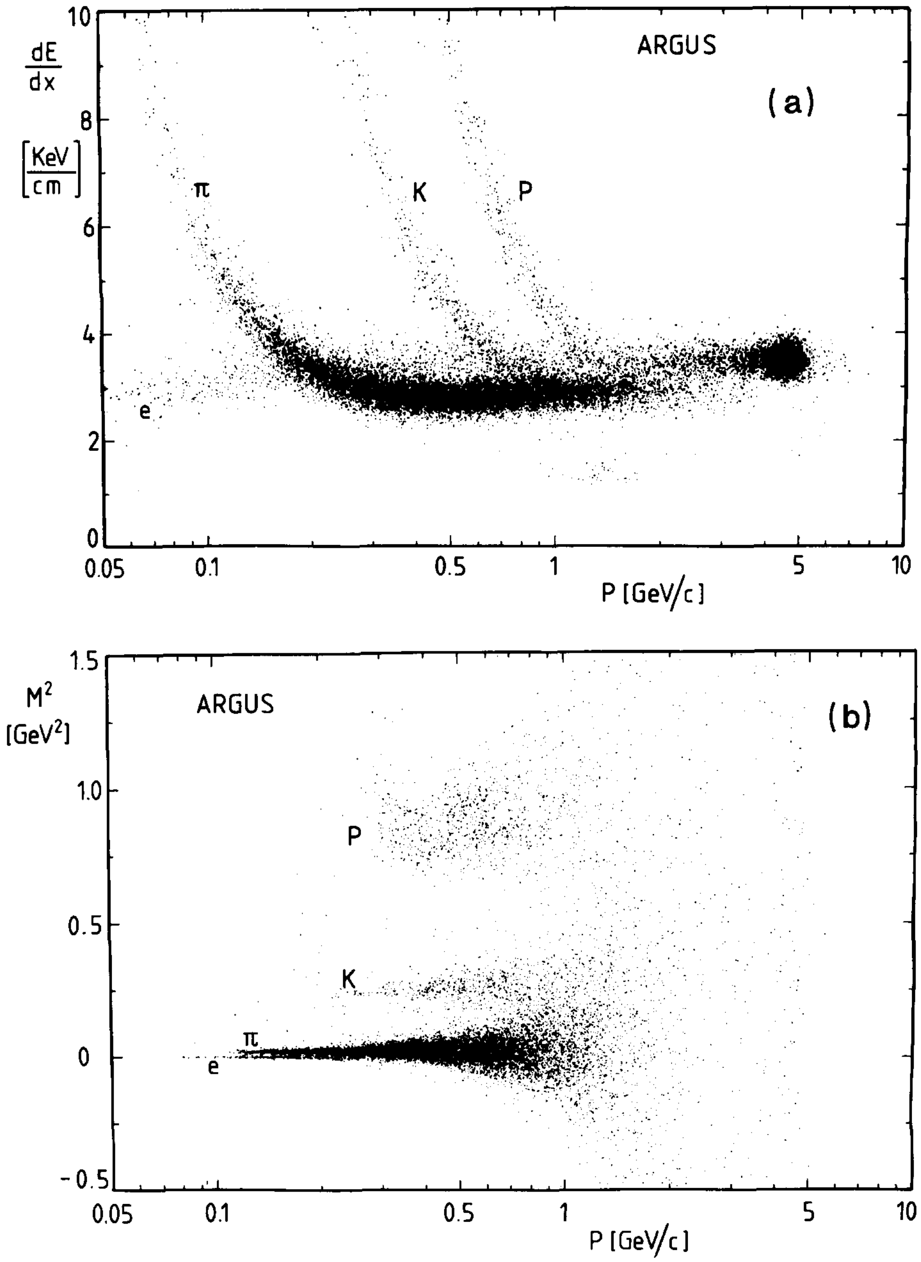

Fig. 1. (a) Scatter plot of dE/dx versus $\log(p)$ in the ARGUS drift chamber. The bands attributed to e, π, K, and p are indicated. (b) Scatter plot of $(\text{mass})^2$ versus $\log(p)$ obtained using the ARGUS TOF system. The bands for e, π, K, and p are indicated.

ence $\Delta M = M(D^0\pi^+) - M(D^0)$, and allows the cascade decay events to be seen in the presence of large combinatorial background. To search for the decays

$$D^{*+} \to D^0\pi^+ \quad \hookrightarrow K^-\pi^+, \qquad (1)$$

and

$$D^{*+} \to D^0\pi^+ \quad \hookrightarrow K^-\pi^+\pi^+\pi^-, \tag{2}$$

we have formed all invariant mass combinations of K^- candidates with two and four charged π combinations of net charge +2. The mass hypothesis probability cut was set $\geqslant 0.01$. This very loose probability cut reduces the background considerably while losing only a negligible amount of the signal.

In figs. 2a and 2c we show the mass difference distributions for $M(K^-\pi^+\pi^+) - M(K^-\pi^+)$ and $M(K^-\pi^+\pi^+\pi^+\pi^-) - M(K^-\pi^+\pi^+\pi^-)$. The subcombina-

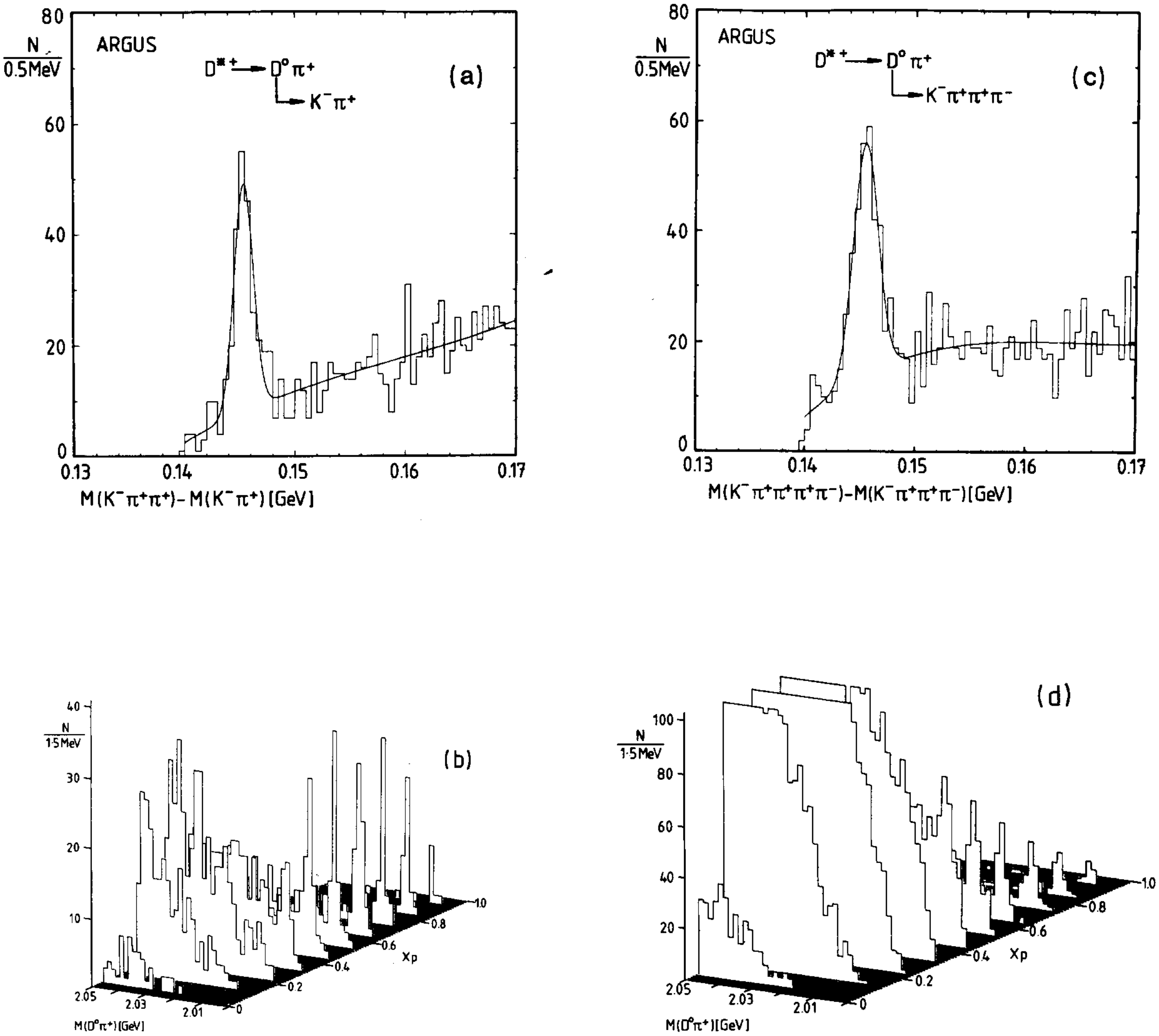

Fig. 2. (a) The mass difference distribution for channel (1). A mass selection, $1825 \leqslant M(K^-\pi^+) \leqslant 1905$ MeV was applied. D^{*+} production is evident. The solid line represents a gaussian fit with a polynomial background. The fit gives $\sigma = (0.87 \pm 0.12)$ MeV and $M(D^{*+}) - M(D^0) = (145.41 \pm 0.10)$ MeV. (b) The effective mass distribution of $(D^0\pi^+)$ versus the fragmentation variable x_p for channel (1). The $K^-\pi^+$ combinations were constrained to the known D^0 mass in a kinematic fit. (c) As (a), but for channel (2). A mass selection of $1835 \leqslant M(K^-\pi^+\pi^+\pi^-) \leqslant 1895$ MeV and a cut of $x_E \geqslant 0.6$ were applied, where $x_E = 2E(D^*)/\sqrt{s}$. A fit gives $\sigma = (1.11 \pm 0.11)$ MeV and $M(D^{*+}) - M(D^0) = (145.51 \pm 0.11)$ MeV. (d) As (b), but for channel (2).

tions $K^-\pi^+$, in the former, and $K^-\pi^+\pi^+\pi^-$ in the latter, were required to be in the range of the D^0 mass, specifically $1825 \leqslant M(K^-\pi^+) \leqslant 1905$ MeV, and $1835 \leqslant M(K^-\pi^+\pi^+\pi^-) \leqslant 1895$ MeV.

In both distributions there is a clear signal for the cascade decay $D^{*+} \to D^0\pi^+$. The fitted mass difference for channels (1) and (2) are 145.41 ± 0.10 and 145.51 ± 0.11 respectively. This yields an average of:

$$\Delta M = M(D^{*+}) - M(D^0) = (145.46 \pm 0.07 \pm 0.03)\text{MeV}.$$

This is in good agreement with the world average [6] of (145.41 ± 0.24) MeV, and is considerably more precise. The estimated systematic error of 0.03 MeV includes the effect of the 0.2% uncertainty in the magnetic field calibration, of uncertainties in corrections for energy losses between vertex and drift chamber, and of varying the assumed form of the background shape.

The invariant mass distribution for $K^-\pi^+$ and $K^-\pi^+\pi^+\pi^-$ contain essentially the same information as that contained in the mass difference distributions shown in figs. 2a and 2c, and are not shown here. However, fitting these mass distributions with a gaussian line shape, plus a third order polynomial background confirms our overall mass scale and our knowledge of the experimental mass resolution. The fits yielded 191 ± 19 events at a fitted mass of (1864 ± 4) MeV in channel (1) and 216 ± 21 events at a fitted mass of (1866 ± 3) MeV in channel (2). The masses in both channels agree well with previously reported [6] values of the D^0 mass. The widths of the signals are in very good agreement with the Monte Carlo predictions of 30 MeV in channel (1) and 20 MeV in channel (2).

The fragmentation of a c quark into a charmed meson is expected to result in a hard momentum spectrum, while background invariant mass combinations should have a much softer momentum spectrum. In figs. 2(b) and 2(d) we show plots of the $D^0\pi^+$ invariant mass spectrum against the fragmentation variable x_p, where $x_p = p_{D^*}/p_{\text{Max}}$ with $p_{\text{Max}} = (E^2_{\text{beam}} - M^2_{D^*})^{1/2}$. We note that both x_p and the energy scaling variable $x_E = E_{D^*}/E_{\text{beam}}$ have been used in the literature. These are approximations to the light-core variable $z = (E + p_{\parallel})_{\text{hadron}}/(E + p)_{\text{quark}}$, equivalent in the scaling limit [7]. The variable x_p used here has the additional virtue of spanning the same range [0, 1] for all experiments, regardless of the center of mass energy. The alternative choice, x_E, has a different threshold for our result and for those from PETRA and PEP. In producing these invariant mass distributions the $K^-\pi^+$ and $K^-\pi^+\pi^+\pi^-$ combinations were constrained to the D^0 mass and a kinematic fit was performed. The number of D^{*+} events in each x_p bin was extracted by fitting a gaussian with width fixed to the Monte Carlo prediction of the mass resolution, plus a polynomial background, to the $D^0\pi^+$ mass spectrum in each x_p bin.

Acceptances were calculated for both channels by means of a Monte Carlo simulation. Events were generated for the process $e^+e^- \to c\bar{c}$ and allowed to fragment into D^{*+} according to the Field and Feynman model [8]. The resulting final state particles were tracked through a simulation of the ARGUS detector and analysed with the standard program chain. The calculated acceptances as a function of x_p range from 0.13 at x_p of 0.25 to 0.33 at x_p of 0.95 for channel (1). The corresponding range of acceptances for channel (2) is from 0.08 to 0.21.

We have estimated the systematic uncertainty in the acceptance calculation by comparing the geometrical acceptance for events of this kinematical configuration with the acceptance estimate from the full Monte Carlo simulation. This comparison results in an estimate of 0.78 for the single track efficiency. A sample of representative multihadron events was also scanned by physicists. For events within the cuts for this analysis the single track efficiency was estimated to be 0.82. This leads to a 16% systematic uncertainty on the acceptance for channel (1) and 28% for channel (2). However, in determining the ratio of the branching ratios of the two channels the uncertainty on the relative acceptances reduces to 10.5%.

After acceptance correction the relative branching ratio of the two channels is:

$$\text{Br}(D^0 \to K^-\pi^+\pi^+\pi^-)/\text{Br}(D^0 \to K^-\pi^+)$$

$$= 2.17 \pm 0.28 \pm 0.23.$$

This is a significant improvement in precision compared to the previous world average of 1.92 ± 0.67 [6].

Above x_p of 0.5 the cross section times branching ratios ($\sigma \cdot \text{Br}$) for channels (1) and (2) are (14.0 ± 1.3 ± 2.6) pb and (30.3 ± 2.7 ± 9.0) pb respectively. The systematic errors include the acceptance uncertainty added in quadrature with an uncertainty on the lumi-

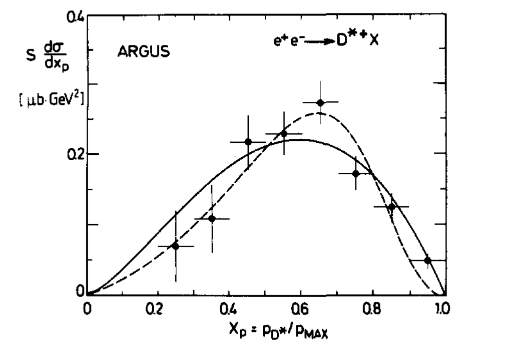

Fig. 3. $s\,d\sigma/dx_p$ for the D^{*+} based on the two channels. The error bars are statistical only. The dotted and solid curves result from fits of the expressions (3) and (4) respectively.

nosity measurement of 10%. The production rates of the D^{*+} on the Υ, Υ', and the continuum are proportional to the luminosity divided by the square of the center of mass energy. Thus there is no indication, at the present level of statistics, of any D^{*+} production from the resonances.

From the number of D^{*+} events extracted as a function of x_p we have produced the D^{*+} fragmentation function, by combining the data in both channels. The result, corrected for acceptance, is shown in fig. 3. In determining the absolute normalization of this distribution we have used the values of ref. [6] for the branching ratios of $D^{*+} \to D^0\pi^+$ and $D^0 \to K^-\pi^+$, combined with the above value for the ratio of branching ratios. It is interesting to compare this measured distribution to forms predicted theoretically. We have compared the data to two typical models, that of Peterson et al. [9] where

$$s\,d\sigma/dx_p \sim x_p^{-1}[1 - 1/x_p - \epsilon/(1 - x_p)]^{-2}, \qquad (3)$$

and that of Kartvelishvili et al. [10] where:

$$s\,d\sigma/dx_p \sim x_p^{\alpha}(1 - x_p). \qquad (4)$$

No attempt has been made to correct these expressions for the effects of photon or gluon radiation.

The fits for forms (3) and (4) are shown as the dotted and full curves in fig. 3. The best fitted parameters are $\epsilon = 0.19 \pm 0.03$ with $\chi^2 = 19.2$ for 6 degrees of freedom, and $\alpha = 1.5 \pm 0.2$ with $\chi^2 = 7.4$ also for 6 degrees of freedom. Our data favour the form (4). They are less consistent with the form in (3), the main disagreement is in the x_p bin from 0.9 to 1.0. A change of variable from x_p to $x_E = 2E(D^*)/\sqrt{s}$ or the inclusion of radiative corrections does not change this conclusion.

The measurement of the D^* fragmentation function presented here represents an improvement in statistical precision over results from CLEO in a similar energy range and from PETRA and PEP at higher energies [1]. Within the statistical uncertainties our measurement is in agreement with these results. Comparison of published measurements can be found in the literature [7].

Using the fitted form of the fragmentation function due to Kartvelishvili we have evaluated $\sigma \cdot$Br for channels (1) and (2) extrapolated to $x_p = 0$. The results are respectively $(23.6 \pm 2.2 \pm 4.7)$ pb and $(51.0 \pm 4.6 \pm 15.5)$ pb.

We have looked for the effect of $D^0 - \overline{D^0}$ mixing in our data. A summary of previous upper limits was given in a recent publication [11]. The method used here is based on the search for wrong signed D^0 decay of the D^{*+} in channel (1), that is the presence of D^{*+}-like events in the mass conbination $K^+\pi^-\pi^+$. Since the main source of background is particle misidentification in the correct sign decays, we have chosen to work with a highly restricted sample. The only changes from the above selection criteria were to increase the probability cut from 0.01 to 0.10 and to require $x_E \geqslant 0.7$. The two mass difference plots obtained are shown in fig. 4. There are 30 events in the

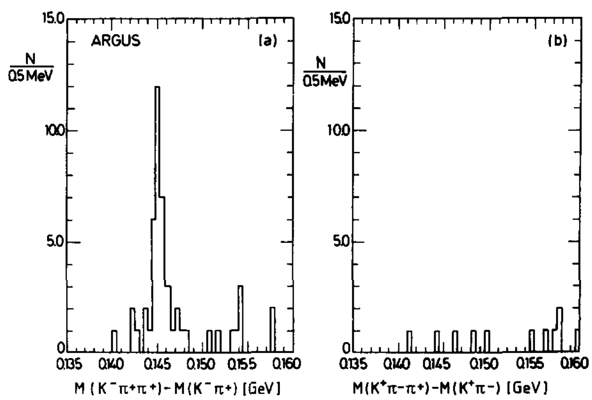

Fig. 4. (a) The distribution of ΔM for the correct charge combinations $M(K^-\pi^+\pi^+) - M(K^-\pi^+)$. (b) The distribution of ΔM for the wrong charge combinations $M(K^+\pi^-\pi^+) - M(K^+\pi^-)$.

correct sign mode, and 2 events in the wrong sign mode, where 2 background events were expected. This observation yields an 11% upper limit for $D^0 - \bar{D}^0$ mixing at 90% confidence level.

In summary, we have determined more precise values for the mass difference of the D^{*+} and D^0 and for the relative branching ratio of D^0 into $K^-\pi^+$ and $K^-\pi^+\pi^+\pi^-$ than previously known. The $D^0 - \bar{D}^0$ mixing is found to be smaller than 11%. Finally, the fragmentation function of the D^{*+} meson is in very good agreement with the form $x^\alpha (1 - x)$, while its agreement with the widely used Peterson form is less good.

It is a pleasure to thank E. Michel, W. Reinsch and Mrs. U. Djuanda for their competent technical help in running the experiment and analyzing the data. We thank Dr. H. Nesemann, Dr. K. Wille and the DORIS group for the good operation of the storage ring. The visiting groups wish to thank the DESY directorate for the support and kind hospitality extended to them.

References

[1] P.A. Rapidis et al., Phys. Lett. 84B (1979) 507;
J.M. Yelton et al., Phys. Rev. Lett. 49 (1982) 430;
C. Babek et al., Phys. Rev. Lett. 49 (1982) 610;
Tasso Collab., M. Althoff et al., Phys. Lett. 126B (1983) 493;
P. Avery et al., Phys. Rev. Lett. 51 (1983) 1139;
S. Ahlen et al., Phys. Rev. Lett. 51 (1983) 1147;
W.B. Atwood et al., Proc. SLAC Summer Institute on Particle physics (1983) p. 607.

[2] Argus Collab., H. Albrecht et al., Phys. Lett. 134B (1984) 137.

[3] M. Danilov et al., Nucl. Instrum. Methods 217 (1983) 153.

[4] R. Heller et al., The ARGUS time-of-flight system, to be published in Nucl. Instrum. Methods (1985).

[5] S. Nussinov, Phys. Rev. Lett. 35 (1975) 1672;
G.J. Feldman et al., Phys. Rev. Lett. 38 (1977) 1313.

[6] Particle Data Group, Rev. Mod. Phys. 56 (1984) S1.

[7] J. Dorfan, Proc. 1983 Intern. Symp. on Lepton and photon interactions at high energies (Cornell University, 1983) p. 686.

[8] R.D. Field and R.P. Feynman, Nucl. Phys. B136 (1978) 1.

[9] C. Peterson et al., Phys. Rev. D27 (1983) 105.

[10] V.G. Kartvelishvili et al., Yad. Fiz. 38 (1983) 1563.

[11] R. Bailey et al., Phys. Lett. 132B (1983) 237.